Image Denoising Using the Hurst Exponent: A Fusion Based Approach

Corina Nafornita
Communications Department
Politehnica University of Timisoara
Timisoara, Romania
corina.nafornita@upt.ro

Alexandru Isar
Communications Department
Politehnica University of Timisoara
Timisoara, Romania
alexandru.isar@upt.ro

Ioan Nafornita
Communications Department
Politehnica University of Timisoara
Timisoara, Romania
ioan.nafornita@upt.ro

***Abstract*—We propose in this paper a denoising method based on the texture roughness appreciation, realized using a semi-local estimation of the Hurst exponent. The estimation is made in the Dual Tree Complex Wavelet domain, by using techniques such as the least squares or the lasso. The Hurst exponent is used to correct the energy distribution of the wavelet coefficients. This removes the noise in homogeneous areas but can oversmooth the edges. In order to overcome this, we propose a fusion based approach, based on the observation that the noise is less visible on the edges. Both the denoised image as well as the original image are weighted by images that depend on the Hurst parameter, such that the edges are less degraded, and the correction is applied predominantly in the homogeneous areas. Our simulation results are promising for images containing both smooth areas as well as edges for the fusion based approach.**

Keywords—denoising, image, texture, edges, Hurst exponent, Dual Tree Complex Wavelet Transform

I. INTRODUCTION

Digital images can be affected by noise, which is an unwanted component in the image, and thus the quality of these images is degraded [1]. The grain noise in photographic films is modelled as Gaussian or Poisson. Many images are corrupted by salt and pepper noise. Other noises are quantization noise and speckle (as for example the case of SAR or SONAR images). An important task is finding a denoising algorithm, such that it diminishes the noise power, while preserving the image features (edges and fine details). There are several such algorithms, some operating in the spatial domain, while others in the frequency domain.

Our aim is to propose a denoising system for images with textural content, based on the Hurst parameter. The Hurst estimation is made in the Dual Tree Complex Wavelet domain, by using techniques such as the least squares or the lasso. The Hurst exponent is used to correct the energy of the wavelet coefficients distribution. This removes the noise in homogeneous areas, but may result in oversmoothed edges, which can be visible to the human eye.

In this paper, we propose a fusion based approach, based on the observation that the noise is less visible on the edges. The algorithm will fuse two images: the denoised one and the original one. The denoised image is weighted by an image dependent on the Hurst estimate, such that the smooth areas of the image are denoised. Similarly, the original image is weighted by an image dependent on the Hurst estimate, such that the edges are less degraded. Thus, the correction is applied predominantly in the homogeneous areas and less in the edges of the image. Our simulation results are promising for images containing both smooth areas as well as edges for the fusion based approach.

The paper is organized as follows: Section 2 presents our motivation, Section 3 presents the algorithm proposed, Section 4 shows the simulation results, while the last section is dedicated to conclusions and future research.

II. MOTIVATION

An important feature of an image is the roughness; its estimation makes possible various applications, such as denoising or segmentation [2-7]. The roughness of a surface in a natural image can be estimated by the Hurst exponent, because the natural images follow a fractional Brownian motion (fBm) model [8]. The wavelet coefficients follow a power law, from which the Hurst exponent is obtained by using simple least squares, LS [2, 5] or lasso [3-5].

In Fig. 1, we give an example of a synthetic texture, generated by using same statistical model but three different values of the Hurst parameter. The area with the largest Hurst value (one) is the most homogeneous one, while the area with the smallest Hurst value (1/3) is the roughest one. It is clear that the Hurst exponent describes smoothness/roughness in an image. We notice that in this case, there is no predominant direction in the texture, meaning it is isotropic [9].

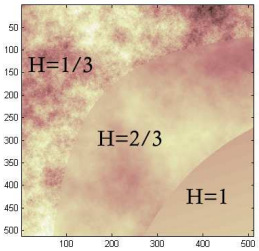

Fig. 1. Synthetic isotropic texture generated using piecewise-varying Hurst parameter.

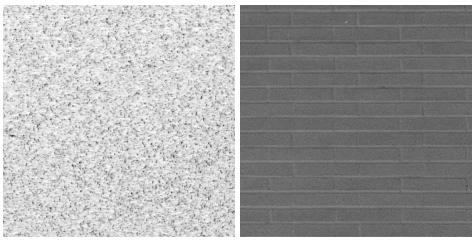

Fig. 2. Texture images from the Brodatz database, characterized by different Hurst parameters - sand (1.5.04) vs brick wall (1.5.06). The first texture is isotropic while the second one is anisotropic.

In Fig. 2, there are examples of some real texture images from the USC-SIPI database [10], which are isotropic (see left image) or anisotropic, with horizontal predominant direction of the texture (see right image). In a natural image, we may encounter smooth areas as well as edges (such as in second image in Fig. 2). The noise is more visible in the

978-1-6654-5150-5/22/$31.00 ©2022 IEEE

smooth areas, than it is in the edges. It is important for the denoising method to affect the edges as less as possible. Hence, our method proposes to apply denoising on the smooth areas, by weighing the denoised result with the Hurst estimated image. In order to retain the edges, the original image is weighted by an image also dependent on the Hurst image. The two images are then fused.

III. Proposed Method

In a natural image, we can assume a patches model (whereby the Hurst exponent varies in a piecewise constant manner) [3], such as in Fig. 1. The Hurst estimation is a difficult task, especially when the acquired image is perturbed by noise [3]. Several methods have been proposed for Hurst estimation in recent years [2-7].

In this paper, we use the estimation of the Hurst parameter in the Dual Tree Complex Wavelet Transform (DTCWT) domain, as proposed in [5]. The method can use Least squares or lasso. The denoising method consists in the estimation of the Hurst exponent in the wavelet domain, followed by correction of the wavelet coefficients (to improve the distribution of their energy) for the entire image.

The log-energy of the wavelet coefficients of fBm processes is proportional with $2k(H+1)$: $E\left|\left(\mathrm{W}f\right)(\cdot,k,m)\right|^2 \propto 2^{2k(H+1)}$, where W is the wavelet transform, m is the subband, k is the level of decomposition, and H is the Hurst exponent. The log-energies of the coefficients are taken at location i:

$$y_k[i] = k\beta_2[i] + \beta_1[i], \tag{1}$$

where $y_k[i] = \log_2 E_{k,m}[i]$. The slope β_2 and the intercept β_1 are estimated on all wavelet decomposition levels, using different algorithms: least squares (LS), or generalized least absolute shrinkage and selection operator (lasso) to perform a spatial regularization, as described in [5]. One can use finest k_- to coarsest k_+ scale levels, with $k_- = 1$ and $k_+ = J = \log_2(M)$, $M*M$ being the size of the image. It was observed that in practice it is better to avoid the highest and the lowest resolution levels. Thus, the estimation is made on levels $k = K+1,\ldots,J-1$ using LS as well as lasso (discarding from the estimation K highest resolution levels and the lowest resolution level).

This is followed by the denoising step on K finest resolution levels. To ensure computational speed, we downsample the subband images by a factor of 16*16. The energy of the wavelet coefficients is then corrected if it's above the estimated value.

As such, a denoised image is obtained. After experiments, it was noted that denoising may result in degradation of the edges. Smooth areas are associated with large Hurst parameters, while edges are usually associated with smaller Hurst parameters. Therefore, we propose a fusion of two images, I_1 and I_2:

$$I_1 = H_n \cdot D \tag{2}$$

$$I_2 = (1 - H_n) \cdot I \tag{3}$$

$$I_f = I_1 + I_2 \tag{4}$$

where H_n is the normalized Hurst image (to range from 0 to 1), D represents the denoised image and I the original noisy image. The result of the fusion-based denoising method is I_f.

It is to be noted that this method assumes the image contains both rough patches that have a small value of the Hurst parameter, as well as smooth patches, with large values of the Hurst parameter.

IV. Simulation Results

In our simulations, we have used different types of images, both synthetic and real images, affected by AWGN noise. As for the parameters used, we have performed the DTCWT transform on J = 9 levels, for images of size 512*512, and for the denoising step, we have used K=2 highest resolution levels. The downsampling step is 16. In all experiments, we have considered that the noise affecting the image is additive white Gaussian noise, with variance 0.005.

One experiment is done on a synthetic texture of size 512*512, with one area homogeneous and isotropic and another one with directional edges.

In Fig. 3, we show this image, together with the Hurst exponents estimated by the two of the methods considered: LS and Lasso. We observe that the Hurst exponent based on Lasso is smoother than the one based on LS.

In Fig. 4, we show the noisy image, together with the Hurst exponents using LS and Lasso estimation.

In Fig. 5, we present the result of the denoising procedure. The denoised images for the synthetic texture image are as follows: the denoised image D using the LS Hurst based denoising; the fused result $I_{f,LS}$, using Hurst exponent estimated by LS, and finally the fused result $I_{f,lasso}$, using Hurst exponent estimated by Lasso.

TABLE I. Results Obtained for the Synthetic Image affected by AWGN Noise with variance 0.005, for the Proposed Methods

Method	Results for synthetic image		
	***PSNR* (dB)**	***SNR* (dB)**	***SSIM* (%)**
Noisy input image	23.08	16.93	50.86
LS Hurst based denoising	24.06	17.73	72.56
Fusion based approach (LS)	**26.97**	**20.73**	80.79
Lasso Hurst based denoising	24.03	17.70	72.45
Fusion based approach (Lasso)	26.89	20.65	**82.23**

In Table I, we give the results for the synthetic image, in terms of PSNR, SNR and SSIM. The noisy image has a SNR of 16.93 dB. The results obtained for the first step (LS/Lasso Hurst based denoising) show an increase of almost 1dB for the PSNR and SNR values, and over 20% increase for SSIM.

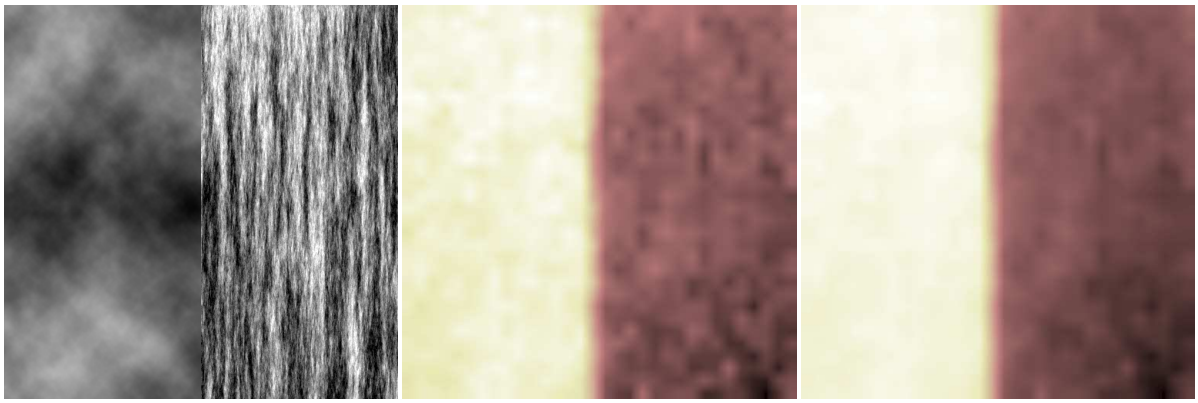

Fig. 3. Syntethic texture image, with two areas, of different Hurst parameter values (left area is smooth, while right area contains edges). Left to right: original image; Hurst exponent estimated using LS; Hurst exponent estimated using Lasso.

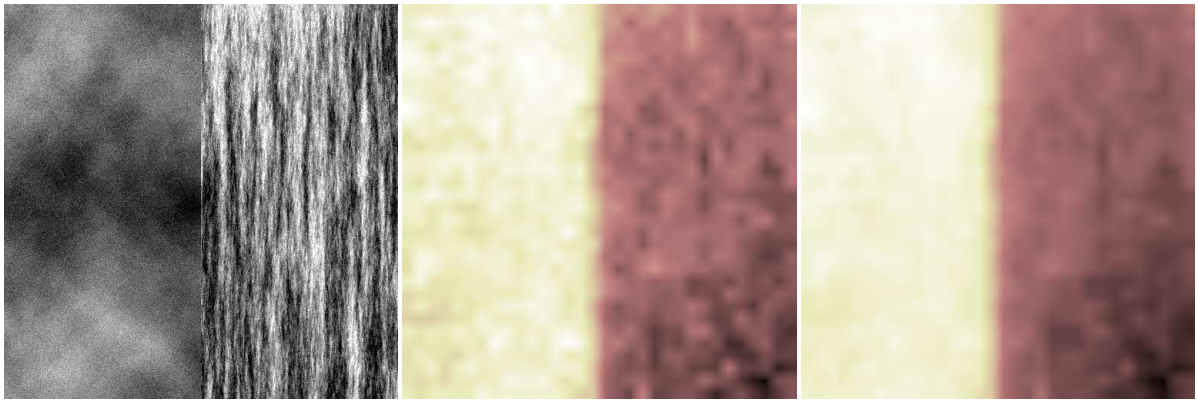

Fig. 4. Syntethic texture image, affected by AWGN noise, with variance 0.005. Left to right: noisy image; Hurst exponent estimated using LS; Hurst exponent estimated using Lasso.

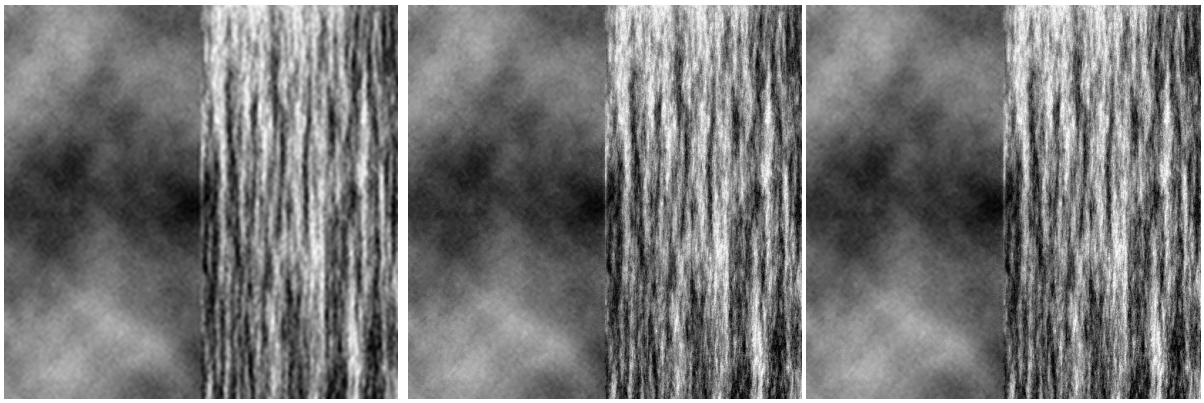

Fig. 5. Denoised images for the syntethic texture image. Left to right: the denoised image D using the LS Hurst based denoising; the fused result $I_{f,LS}$, using Hurst exponent estimated by LS; the fused result $I_{f,lasso}$, using Hurst exponent estimated by Lasso.

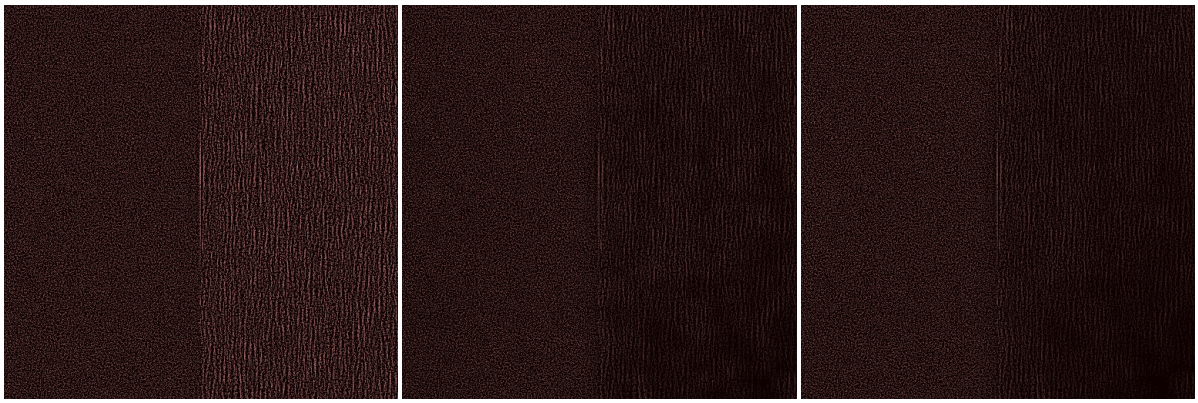

Fig. 6. Difference between the noisy image and the resulting denoised images. Left to right: LS Hurst based denoising; denoising by fusion using Hurst exponent estimated by LS; denoising by fusion using Hurst exponent estimated by Lasso.

The results obtained for the second step (fusion using LS/Lasso Hurst) show an increase of almost 4 dB for the PSNR and SNR values, and around 30% increase for SSIM.

In terms of PSNR and SNR, the best results are obtained for the fusion method by LS estimated Hurst exponent. In terms of SSIM, the best results are obtained for the fusion method by Lasso estimated Hurst exponent.

It is observed from Fig. 5, that the LS Hurst based denoising reduces the noise in the homogeneous area, but also oversmoothed the area containing edges.

In the fusion result, the treatment of the edges is greatly improved, as observed in Fig. 5. The treatment of the edges is observed also from Fig. 6, which shows the difference between the noisy image and the resulting denoised images for: LS Hurst based denoising; denoising by fusion using Hurst exponent estimated by LS; denoising by fusion using Hurst exponent estimated by Lasso. In the first case, the noise is reduced from the smooth area, but also edges, resulting in an oversmoothing of the edges. In the second and third case, the noise is reduced predominantly from the homogeneous area, and much less in the area containing edges. This is also noticed from the PSNR, SNR and SSIM values that are the highest, compared to the other methods. The fusion result outperforms the result obtained for the first step of denoising. Same observations are true for the Lasso results.

In the following, we present the second scenario, a real image affected by AWGN noise, same variance of 0.005. We chose the Barbara image, due to its diverse content of both homogeneous areas as well as edges.

Fig. 7. Barbara image used in the second scenario. Left to right: original; noisy version for AWGN noise with variance 0.005.

The original image and noisy version are shown in Fig. 7. In Fig. 8, we present the result of the denoising procedure. The denoised images for Barbara are as follows: the denoised image D using the LS Hurst-based denoising and the fused result $I_{f,LS}$, using Hurst exponent estimated by LS.

In Table II, we give the results for Barbara image, in terms of PSNR, SNR and SSIM. The noisy image has a SNR of 17.24 dB. The results obtained for the first step (LS/Lasso Hurst based denoising) show an increase of less than 1dB for the PSNR/SNR values, and almost 15% increase for SSIM.

The results obtained for the second step (fusion using LS/Lasso Hurst) show an increase of almost 3 dB for the PSNR and SNR, and over 16% increase for SSIM.

The best results are obtained for the fusion method by LS estimated Hurst.

It is observed from Fig. 8, that the LS Hurst based denoising reduced the noise in the homogeneous area, but also oversmoothed the area containing edges (such as the pants and the scarf). In the fusion result, the treatment of the edges is greatly improved.

This is seen also in Fig. 9, which gives the difference between the noisy image and the denoised images for: LS Hurst based denoising and denoising by fusion using LS Hurst exponent. In the first case, the noise is reduced from the smooth area, but also edges, resulting in an oversmoothing. In the fusion case, the noise is reduced predominantly from the homogeneous areas, and less in the edges' areas. The fusion method outperforms the result obtained for the first step of denoising.

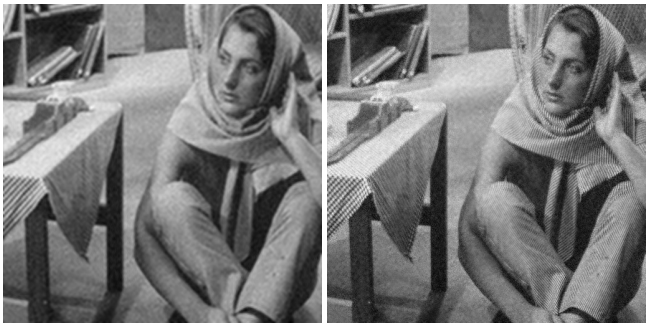

Fig. 8. Denoised images for the Barbara image. Left to right: the denoised image D using the LS Hurst based denoising; the fused result $I_{f,LS}$, using Hurst exponent estimated by LS.

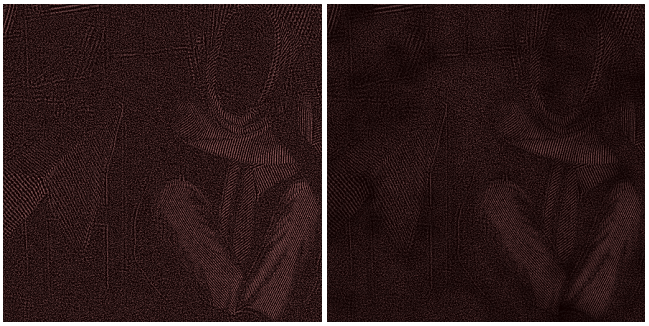

Fig. 9. Difference between the noisy image and the resulting denoised images. Left to right: LS Hurst based denoising; denoising by fusion using Hurst exponent estimated by LS.

TABLE II. RESULTS OBTAINED FOR THE BARBARA IMAGE AFFECTED BY AWGN NOISE WITH VARIANCE 0.005, FOR THE PROPOSED METHODS

Method	**Results for Barbara image**		
	***PSNR* (dB)**	***SNR* (dB)**	***SSIM* (%)**
Noisy input image	23.05	17.24	51.48
LS Hurst based denoising	23.86	17.90	65.60
Fusion based approach (LS)	**25.81**	**19.90**	**67.13**
Lasso Hurst based denoising	23.84	17.89	65.50
Fusion based approach (Lasso)	25.76	19.86	66.17

In order to test the treatment on the edges, we also applied a Canny edge detector for all images: original, noisy, denoised and denoised using the fusion methods. Edge thresholds are automatically chosen, relative to the highest value of the gradient magnitude of the image. The edge maps are shown for Barbara image in Fig. 10.

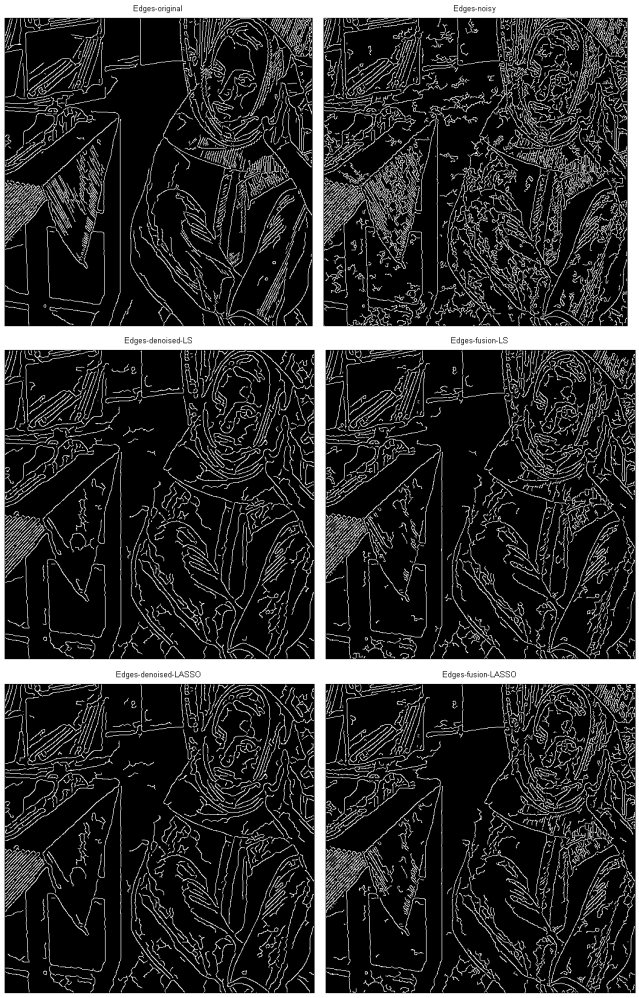

Fig. 10. Edge maps for Barbara image, using Canny detector. From left to right, top to bottom, we show the edge maps for: original image; noisy image; LS Hurst based denoised image; fusion based approach denoised image with LS; Lasso Hurst based denoised image; fusion based approach denoised image with Lasso.

TABLE III. EDGE TREATMENT RESULTS FOR CANNY EDGE DETECTOR

Image/Method	**Edges (%)**	
	Synthetic image	***Barbara***
Original image	10.4351	10.2592
Noisy image	10.9428	15.1299
LS denoising	8.0746	9.0157
LS fusion denoising	10.0315	10.0105
Lasso denoising	8.0635	9.0340
Lasso fusion denoising	10.1925	10.5022

The percentage of pixels detected as edges are given in Table III, for both test images. Analyzing Fig. 10 and Table III, we see that due to the noise, the number of edges increases, compared to the original image (more in the Barbara case than in the synthetic image case, see Table III). This decreases after denoising, as expected, and it increases after the fusion step. In fact, after denoising, it decreases below the original image edge percentage, as a consequence of oversmoothing. The fusion will bring the value closer to the original image. The Lasso fusion based method increases the number of edges more than the LS fusion based method.

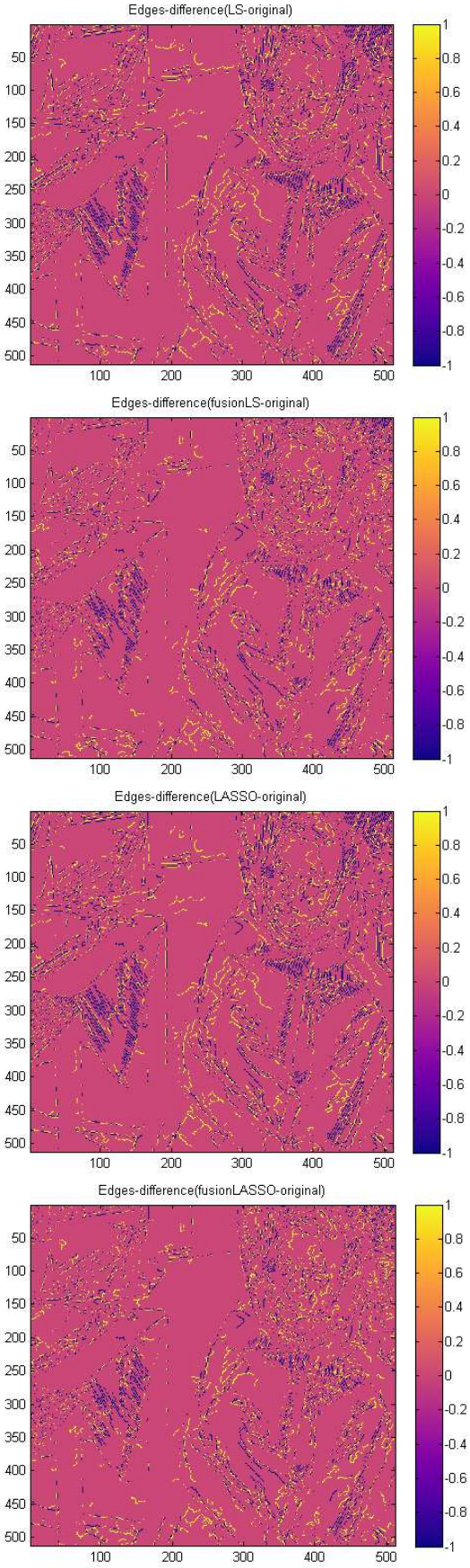

Fig. 11. Difference edge maps for Barbara. The difference is between the denoised image edge map and the original image edge map, respectively. From top to bottom: LS Hurst based denoised image; fusion based approach denoised image with LS; Lasso Hurst based denoised image; fusion based approach denoised image with Lasso.

We checked also the errors introduced by the denoising method, for example if a false edge appears after the denoising (false positive), or if an edge is no longer detected (false negative). Again, we present the edges difference map for the Barbara image, in Fig. 11. The difference maps have 0 values shown in pink (no errors), 1 values (corresponding to a pixel of a false edge/false positive, shown in yellow) and -1 values (a pixel of an undetected edge/false negative, shown in purple). We notice in Fig. 11 by checking the purple lines (-1 values) what texture pixels have been "erased" by the denoising method. For example, the areas of the pants or scarf have less values of -1 for the fusion based method, which is consistent with our previous results.

The errors are given in Table IV for both images (minimum values are shown in bold). In both cases, the fusion step will decrease the errors. The LS fusion produces less false positives, while the Lasso fusion produces less false negatives.

TABLE IV. EDGE TREATMENT ERRORS FOR CANNY EDGE DETECTOR

Method	**Errors (%)**			
	Synthetic image		***Barbara***	
	false positive	***false negative***	***false positive***	***false negative***
LS Hurst based denoising	4.2599	6.6204	4.3327	5.5763
Fusion based approach (LS)	**2.3518**	2.7554	**4.0295**	4.2782
Lasso Hurst based denoising	4.2603	6.6319	4.3892	5.6145
Fusion based approach (Lasso)	2.4052	**2.6478**	4.2564	**4.0134**

V. CONCLUSIONS

In this paper, we have proposed a denoising method based on the texture roughness appreciation, realized using a semi-local estimation of the Hurst exponent based on [5]. The Hurst exponent estimation is made in the Dual Tree Complex Wavelet domain, by using techniques such as the least squares or the lasso. The Hurst exponent is used to correct the distribution of the energy of the wavelet coefficients. This removes the noise in homogeneous areas, but can oversmooth the edges.

In order to overcome this, we propose a fusion-based approach, based on the observation that the noise is less visible on the edges. Both the denoised image as well as the original image are weighted by images that depend on the Hurst parameter, such that the edges are less degraded, and the correction is applied predominantly in the homogeneous areas. Our simulation results are promising for images containing both smooth areas, as well as edges for the fusion based approach. Our tests, made on both synthetic images as well as real images, affected by AWGN noise, show an improvement of PSNR, SNR, SSIM and the edges areas treatment when applying the fusion based method. Similar with other complex wavelets based denoising methods [12], the proposed method has the capacity to reduce the oversmoothing effect of the edges, in comparison with state of the art denoising methods, as for example the BM3D algorithm [13].

Future research directions are the improvement of the denoising method and extending it to satellite or sonar images, as in [6], as well as a comparison with other edge preserving filters, such as the bilateral filter [14].

REFERENCES

[1] A. C. Bovik, Handbook of Image and Video Processing. Amsterdam: Elsevier Academic Press, 2005.

[2] J. D. B. Nelson and N. G. Kingsbury, "Dual-tree wavelets for estimation of locally varying and anisotropic fractal dimension," IEEE International Conference on Image Processing, pp. 341–344, 2010.

[3] C. Nafornita, A. Isar, and J. D. B. Nelson, "Regularised, semi-local Hurst estimation via generalised lasso and dual-tree complex wavelets," IEEE Int. Conf. Image Proc., 2014, Paris, pp. 2689-2693.

[4] J. D. B. Nelson, C. Nafornita, and A. Isar, "Generalised M-lasso for robust, spatially regularised Hurst estimation," IEEE Global Conf. Signal and Information Processing, Orlando, USA, Dec. 14-16, 2015.

[5] J. D. B. Nelson, C. Nafornita, and A. Isar, "Semi-Local Scaling Exponent Estimation With Box-Penalty Constraints and Total-Variation Regularization," in IEEE Transactions on Image Processing, vol. 25, no. 7, pp. 3167-3181, July 2016.

[6] C. Nafornita, A. Isar, and J.D.B. Nelson, "Denoising of Single Look Complex SAR Images using Hurst Estimation," 12th International Symposium on Electronics and Telecommunications (ISETC), 2016, 26-27 Oct. 2016, Timisoara, Romania, pp 333-338

[7] B. Pascal, S. Vaiter, N. Pustelnik, and P. Abry, "Automated Data-Driven Selection of the Hyperparameters for Total-Variation-Based Texture Segmentation," J Math Imaging Vis 63, pp. 923–952, 2021.

[8] A. Jalobeanu, L. Blanc-Feraud and J. Zerubia, "Natural image modeling using complex wavelets," SPIE Wavelets: Applications in Signal and Image Proc. X, 2003, 480-494.

[9] R. Rosenholtz, J. Malik, "Surface orientation from texture: Isotropy or homogeneity (or both)?," Vision Research, Volume 37, Issue 16, 1997, pp. 2283-2293, ISSN 0042-6989.

[10] "The USC-SIPI Image Database," [Online]. Available: https://sipi.usc.edu/database/. [Accessed Jul. 24, 2022].

[11] I.W. Selesnick, R.G. Baraniuk, and N.G. Kingsbury, "The dual-tree complex wavelet transform," IEEE Signal Proc. Mag., 22, 6, 2005.

[12] C. Nafornita and A. Isar, "Hyperanalytic Wavelets Based Remote Sensing Images Despeckling," 2021 International Symposium on Signals, Circuits and Systems (ISSCS), 2021, pp. 1-4.

[13] K. Dabov, A. Foi, V. Katkovnik, and K. Egiazarian, "Image Denoising by Sparse 3-D Transform-Domain Collaborative Filtering," in IEEE Transactions on Image Processing, vol. 16, no. 8, pp. 2080-2095, Aug. 2007.

[14] C. Tomasi and R. Manduchi, "Bilateral filtering for gray and color images," Sixth international conference on computer vision (IEEE Cat. No. 98CH36271). IEEE, 1998.